

## Molecular engineering of PETase for efficient PET biodegradation

Tao Wang<sup>a</sup>, Wen-tao Yang<sup>a,1</sup>, Yu-ming Gong<sup>a,1</sup>, Ying-kang Zhang<sup>a,1</sup>, Xin-xin Fan<sup>a,1</sup>, Guo-cheng Wang<sup>a,1</sup>, Zhen-hua Lu<sup>b</sup>, Fei Liu<sup>a</sup>, Xiao-huan Liu<sup>a</sup>, You-shuang Zhu<sup>a,\*</sup>

<sup>a</sup> School of Biological Science, Jining Medical University, Jining, China

<sup>b</sup> College of Chemical and Biological Engineering, Zhejiang University, Hangzhou 310027, China



### ARTICLE INFO

Edited by Bing Yan

**Keywords:**

Polyethylene terephthalate (PET)  
PETase  
Biodegradation  
Carbohydrate-binding module  
Whole-cell catalysts

### ABSTRACT

The widespread utilization of polyethylene terephthalate (PET) has caused a variety of environmental and health problems. Compared with traditional thermomechanical or chemical PET cycling, the biodegradation of PET may offer a more feasible solution. Though the PETase from *Ideonalla sakaiensis* (*Is*PETase) displays interesting PET degrading performance under mild conditions; the relatively low thermal stability of *Is*PETase limits its practical application. In this study, enzyme-catalysed PET degradation was investigated with the promising *Is*PETase mutant HotPETase (HP). On this basis, a carbohydrate-binding module from *Bacillus anthracis* (*Ba*CBM) was fused to the C-terminus of HP to construct the PETase mutant (HLCB) for increased PET degradation. Furthermore, to effectively improve PET accessibility and PET-degrading activity, the truncated outer membrane hybrid protein (FadL) was used to expose PETase and *Ba*CBM on the surface of *E. coli* (BL21with) to develop regenerable whole-cell biocatalysts (D-HLCB). Results showed that, among the tested small-molecular weight ester compounds (*p*-nitrophenyl phosphate (*p*NPP), *p*-Nitrophenyl acetate (*p*NPA), 4-Nitrophenyl butyrate (*p*NPB)), PETase displayed the highest hydrolysing activity against *p*NPP. HP displayed the highest catalytic activity (1.94 μM(*p*-NP)/min) at 50 °C and increased longevity at 40 °C. The fused *Ba*CBM could clearly improve the catalytic performance of PETase by increasing the optimal reaction temperature and improving the thermostability. When HLCB was used for PET degradation, the yield of monomeric products (255.7 μM) was ~25.5 % greater than that obtained after 50 h of HP-catalysed PET degradation. Moreover, the highest yield of monomeric products from the D-HLCB-mediated system reached 1.03 mM. The whole-cell catalyst D-HLCB displayed good reusability and stability and could maintain more than 54.6 % of its initial activity for nine cycles. Finally, molecular docking simulations were utilized to investigate the binding mechanism and the reaction mechanism of HLCB, which may provide theoretical evidence to further increase the PET-degrading activities of PETases through rational design. The proposed strategy and developed variants show potential for achieving complete biodegradation of PET under mild conditions.

### 1. Introduction

Polyethylene terephthalate (PET) has greatly contributed the modern world and is widely applied in various fields because of its excellent mechanical and thermal properties (Carniel et al., 2021; Taniguchi et al., 2019). However, just as every coin has two sides, the increasing accumulation of postconsumer PET waste in the natural environment has posed a serious threat to ecosystems, as PET exhibits exceptional durability and resistance to physicochemical and biochemical degradation (Gao et al., 2022; Tamargo et al., 2022). Therefore, effective strategies to address plastic pollution are urgently needed (Singh Jadaun et al., 2022;

Miri et al., 2022). The enzymatic biodegradation of PET offers a promising alternative to traditional thermomechanical or chemical PET cycling methods (Cao et al., 2022).

To date, various enzymes with efficient PET-degrading activity have been successfully identified; these enzymes are mainly members of the family of carboxylic ester hydrolases (EC 3.1.1.x), and most of them further fall into the subfamily of cutinases (cutinases or the cutinase-like PET-hydrolase), such as TfCut2, Cut190, HiC, and LCC (Ellis et al., 2021; Zumstein et al., 2017; Tamoor et al., 2021; Kumar et al., 2022; Urbanek et al., 2021). These enzymes can cleave PET polymers into diverse monomeric products, including terephthalic acid (TPA), ethylene glycol

\* Correspondence to: No. 669 Xueyuan Road, Donggang District, Rizhao, Shandong province, China.

E-mail address: zhuyoushuang@126.com (Y.-s. Zhu).

<sup>1</sup> These authors contributed equally to this manuscript.

(EG), and mono-(2-hydroxyethyl)terephthalic acid (MHET) (von Haugwitz et al., 2022; Wei and Zimmermann, 2017; Moyses et al., 2021) (Tournier et al., 2020). In 2016, the bacterium *Ideonella sakaiensis* 201-F6 was reported to proliferate on a low-crystallinity (1.9 %) PET film at 30 °C for 40 days and hydrolyse PET with catalysis by two released enzymes (ISF6\_4831 (*IsPETase*) and ISF6\_0224 (*IsMHETase*)) (Yoshida et al., 2016). This led to the rapid development of *IsPETase*, an *IsPETase*-like enzyme, in the field of PET biodegradation (Bell et al., 2022; Son et al., 2020; Cui et al., 2021a; Liu et al., 2022; Shi et al., 2023). However, compared with chitinase or chitinase-like PET-degrading enzymes (e.g., LCC<sup>ICCG</sup> (Tournier et al., 2020), *TfCut*-DM (Yang et al., 2023a)), *IsPETase* exhibits relatively lower PET-degrading activity and thermostability, and these problems have not been fully addressed to satisfy the needs of industrialization. Consequently, further engineering is needed to achieve more efficient PETases.

Various strategies, such as directed evolution (Bell et al., 2022), rational protein design (Liu et al., 2022; Meng et al., 2021; Son et al., 2019; Yin et al., 2022; Lu et al., 2022; Wu, 2021), posttranslational glycan modification (Deng et al., 2023), enhanced secretory expression (Zurier and Goddard, 2023; Shi et al., 2021; Cui et al., 2021b; Seo et al., 2019), and metabolic engineering of the utilized host, have been developed to improve the catalytic performance of PET-degrading enzymes. Moreover, rational construction of PET-degrading enzymes fused to the carbohydrate-binding module (Dai et al., 2021; Ribitsch et al., 2013; Zhang et al., 2013) or to hydrophobic proteins (Puspitasari et al., 2021a, 2021b; Ribitsch et al., 2015) has been confirmed to streamline the binding ability of the fused catalyst to the PET surface and improve the degradation of PET (Weber et al., 2019). In 2019, a *Bacillus anthracis* carbohydrate-binding module (CBM) from family 2 (*BaCBM2*) (Weber et al., 2019), which is the chitin-binding domain of a chitinase enzyme, was identified. In addition, researchers found that *BaCBM2* has a high affinity for crystalline PET and can bind to insoluble polysaccharides, such as cellulose or xylan. Due to these findings, CBMs are promising tools for improving the catalytic performance of several different types of degrading enzymes.

In addition, a strategy that involves cell surface display has been widely used to design renewable biocatalysts by expressing target enzymes on the surface of microbial cells (Gercke et al., 2021; Tissopi et al., 2022; He et al., 2022; Brandenberg et al., 2022). In this system, the target protein is synthesized in microbial cells and then automatically transferred to the cell surface through the cellular secretion system. The target protein is tethered as the fused cargo of the anchor protein on the cell surface. Therefore, the catalytic activities of the target enzyme are maintained on the cell surface, resulting in enhanced stability and reusability (Chen et al., 2021a, 2022; Guo et al., 2023; Pham and Polakovi, 2020). This approach is valuable for designing and constructing cell factories for use as whole-cell catalysts to efficiently biosynthesize biochemicals with high added value.

In this study, a promising PETase, HP (Bell et al., 2022), was further rationally engineered. Fusing HP to *BaCBM2* and functional interaction with the surface of *E. coli* cells were designed to improve the PET-degrading ability of HP. The results showed that the engineered mutants displayed improved degrading activity against PET, which may be an efficient and environmentally friendly whole-cell catalyst for the

biocatalytic degradation of PET.

## 2. Materials and methods

### 2.1. Bacterial strains, plasmids and reagents

HP was employed as the starting point for protein engineering, and the genes in Fig. 1 (such as HP gene (792 bp) (Bell et al., 2022) and the HLCB gene) were all chemically synthesized and codon optimized by Tsingke Biotechnology (<https://tsingke.com.cn/>). The pET22b (+) plasmid was used as the expression vector, and pET30(a) was used for the cell surface display of PETase. *E. coli* DH5α maintained in our laboratory was used as the amplification host, and *E. coli* BL21 (DE3) was employed as the host to heterogeneously express HP and the mutants. All the primers used in this study were chemically synthesized by Sangon Biotech (<https://www.sangon.com/>).

### 2.2. Gene cloning and construction of recombinant bacteria

**Construction of the HP expression vector (p22-HP).** The HP gene was cloned and inserted into the *HindIII* and *BamHI* sites of pET22b (+), resulting in the recombinant plasmid p22-HP.

**Construction of the fusion expression vector for HLCB (p22-HLC).** The carbohydrate-binding module (*BaCBM2*, GenBank: MK349005.1) was fused to the C-terminus of HP to form the recombinant plasmid p22-HLC, which contains a Sec-dependent translocation signal peptide, *pelB*, for secretion. Synthetic oligonucleotides encoding sequences of the flexible peptide linker (GGGGS)<sub>3</sub> were introduced between the *pelB* and HP genes, and also between HP and the carbohydrate-binding module.

**Construction of an *E. coli* display system (p30-D-HLC).** The truncated *fadL* gene (NCBI Reference Sequence: NC\_000913.3) was chemically synthesized and linked to the PETase gene at the C-terminus with flexible peptide linkers (GGGGS)<sub>3</sub>, and the other end of the PETase was linked to *BaCBM2* with the same linkers (GGGGS)<sub>3</sub> (FHLCB, shown in Fig. 1). The constructed gene fragment was then cloned and inserted into the *NdeI* and *XhoI* sites of pET30(a), which formed the recombinant plasmid p30-D-HLC.

All the (recombinant) enzymes carried a C-terminal 6xHis-Tag for rapid purification by affinity chromatography. The sequence-verified plasmids were subsequently transformed into *E. coli* BL21 (DE3)

**Table 1**  
Bacterial strains, plasmids and primers used in this study.

Bacterial strain and plasmid	Relevant characteristic	Source
<b>Strains</b>		
<i>E. coli</i> DH 5α	General cloning host strain	Maintained in our group
<i>E. coli</i> BL21(DE3)	Hosts for the expression of recombinant protein	Maintained in our group
<b>Plasmids</b>		
pET30(a)	Expressing plasmid	Takara
pET22(b)	Expressing plasmid	Takara

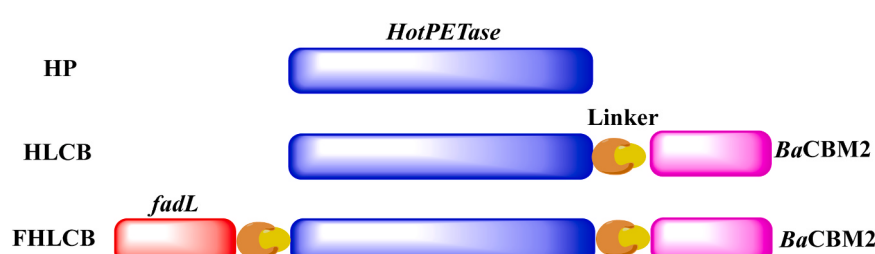


**Fig. 1.** Schematic diagram of the construction of different recombinant gene fragments.

competent cells, resulting in the recombinant strains for the (or secretory) production of heterologous proteins.

### 2.3. Expression, protein quantitation and enzymatic assays

The recombinant strain was cultured overnight and subsequently inoculated into 50 ml of fresh Luria–Bertani (LB) medium supplemented with 50 mg/L kanamycin (for D-HLCB) or 100 mg/L ampicillin (for HP and HLCB) at 37 °C and 200 rpm until the cell density at 600 nm ( $OD_{600}$ ) reached 0.6–0.8. A final concentration of 0.5 mM isopropyl- $\beta$ -D-thiogalactopyranoside (IPTG) was added to the culture before it was incubated at 25 °C and 200 rpm for 10–12 h. The cells were harvested by centrifugation at 6000 × g for 10 min at 4 °C. The pellet was resuspended and washed three times in ice-cold 50 mM Gly-NaOH buffer (pH 9.0), and the cells were resuspended and disrupted by ultrasonic waves. After centrifugation, the crude enzyme solution was purified by a Ni affinity column. The homogeneity of the purified protein was assessed by SDS-PAGE, and the protein concentrations were measured by a Pierce BCA Protein Assay Kit (Shanghai, Thermo Fisher Scientific Co., Ltd.).

It is known that the PETase is capable of catalysing ester bond hydrolysis displaying esterase and lipase activities. Accordingly, the ester bond of different ester compounds hydrolysis could be used for efficient high-throughput screening of PETase variants. Therefore, the PETase activity in this study was determined by using the selected *p*-nitrophenyl palmitate (*p*NPP) as a model substrate (Liu et al., 2022; Ma et al., 2018). The purified protein (or D-HLCB) was added into 190  $\mu$ L of 50 mM glycine-NaOH buffer (pH 9.0) with 10  $\mu$ L of *p*NPP solution (25 mM). After incubation for 30 min at 40 °C, the reaction was terminated by adding 100  $\mu$ L methyl alcohol. The reaction mixture was then analysed by microplate reader at 405 nm (A410). For the D-HLCB, the reaction was terminated by centrifuged to separate D-HLCB from the reaction mixture. The optimum temperatures of variants were determined at temperatures ranging from 40 °C to 70 °C in 50 mM glycine-NaOH buffer (pH 9.0) as mentioned above. For the bio-catalysis of PET film ( $T=0.019$  mm), the film was cut into 0.5 × 0.5 cm<sup>2</sup> pieces (~100 mg) and washed with distilled water, and ethanol, then they are dried at 60 °C for 1 h. The degradation of PET film was performed in 50 mM glycine-NaOH buffer (pH 9.0) with HP, HLCB and D-HLCB in a reaction volume of 20 ml at 40 °C and constant agitation. The reaction was terminated by centrifuged to separate PET film (or D-HLCB) from the reaction mixture, which would be then analysed by microplate reader at 562 nm (A<sub>562</sub>).

One unit of enzyme activity was defined as the release of 1  $\mu$ mol *p*-nitrophenol (*p*-NP) per minute at 40 °C, and the *p*-NP was detected by microplate reader at 405 nm (A<sub>410</sub>). All the experiments were repeated three times.

### 2.4. Molecular docking of substrate recognition and the catalytic mechanism

Molecular docking was performed to determine the molecular basis and mode of action of the PETase using Discovery Studio (DS) 4.0. A homology model of HLCB was generated by MODELER implanted in the DS with 7QVH, 6QFS, 2XBD, 1EXG, and 1E5C as the best templates, and the model with the lowest total PDF energy was identified as the optimal protein structure.

Flexible docking within the DS was used to investigate the docking process during PET degradation. The crystal structure of HotPETase (PDB ID: 7QVH) was used to designate the receptor. The substrate binding site (CC) was defined as the domain lined by the residues Y87, T88, A89, N241, N244, S245, N246, R280, M161, W185, I208, S160, H237, S236, I232, N233 and D206. Residues at Ser160, Asp206 and His237 were identified as the catalytic triad, and the “selected flexible residues” were defined as “CC”. The default settings for the other parameters associated with this process were utilized.

LibDock implanted in the DS was used to investigate the docking process that underlies the PET-binding process of CBM. The homology model of HLCB was used as the receptor, and the binding sphere lined by the residues W288, W323 and W342 was defined with a radius of 20.7037 Å. The ligands (2-HE(MHET)<sub>4</sub>) used in this study were generated with DS.

Force fields (CHARMM) and energy minimization were applied to the target proteins and the ligands, respectively, to guarantee reliable docking analysis. The highest score with a reasonable conformation indicated that the most favourable binding occurred with the target complex structure. The interactions between the ligand and the target in the binding processes were analysed.

All other parameters were left as default values.

## 3. Results and discussion

### 3.1. Screening of the optimal substrate for PETase

To establish an efficient high-throughput screening method for the determination of PET-degrading activity of PETase, substrate screening was firstly carried out to identify the optimal small-molecular weight ester substrates for efficient determination of PETase activity. The results (Fig. 2) indicated that HP displayed hydrolysing activities against all the tested substrates (*p*NPA, *p*NPB, and *p*NPP) at different concentrations; however, HP achieved the best catalytic performance against *p*NPP, which generated the maximum reaction rate and product yields at the same substrate concentration.

Therefore, in the following studies, *p*NPP was selected as a model esterase substrate for the determination of the catalytic performance of PETase mutants.

### 3.2. Effects of reaction temperature on the catalytic performance of HP, HLCB, and D-HLCB

As shown in Fig. 3, it was found that the catalytic activities of HP, HLCB and D-HLCB increased first, and then decreased, which would reach the peaks at 50 °C. Especially, to further increase the reaction temperatures (above 50 °C), the catalytic performance would be significantly inhibited. After ~80 min of incubation at 60 °C, the catalytic activities were decreased by ~45%, 62.8% and 50.3% respectively or HP, HLCB and D-HLCB compared with those incubated at 60 °C.

From Fig. 3(1), the enzymatic hydrolysing activity of *p*-NPP catalysed by HP were explored at various temperatures. At 50 °C, the maximum initial reaction rate was obtained before 80 min. However, the highest conversion rate of 29.87% ( $c_{product}/c_{substrate}$ ) was obtained after ~160 min of incubation. With increasing (or decreasing) incubation temperature to 70 °C, the maximum conversion rate decreased to 8.05% ( $c_{product}/c_{substrate}$ ). This indicated that increasing the temperature accelerated the catalytic rate of the HP; however, with increasing time, increasing the reaction temperature inevitably reduced the catalytic performance of the HP. This result is different from the finding in which HP depolymerized semicrystalline PET more rapidly at ~65 °C (Bell et al., 2022). This difference possibly occurred because at temperatures approaching the reported glass transition temperature ( $T_g$ ) of PET (~60–70 °C) in aqueous solution, the mobile amorphous fraction of the PET polymer could be preferentially accessed by hydrolases and converted into soluble products, resulting in increased PET-degrading activity (Wu, 2021; Pirillo et al., 2023). Results also revealed that reaction temperature above 75 °C was shown to be detrimental to PET conversion caused by rapid recrystallization of PCW-PET (Tournier et al., 2020). Therefore, blind pursuit of higher PET-degrading temperature would display a negative effect on the kinetic turnover. As a result, in this study for the small-molecule substrate *p*NPP, the operating temperature at approximately the  $T_g$  might exert little stimulatory effect on the substrate-degrading enzymes.

A comparison of the reactions between HP, HLCB and D-HLCB at

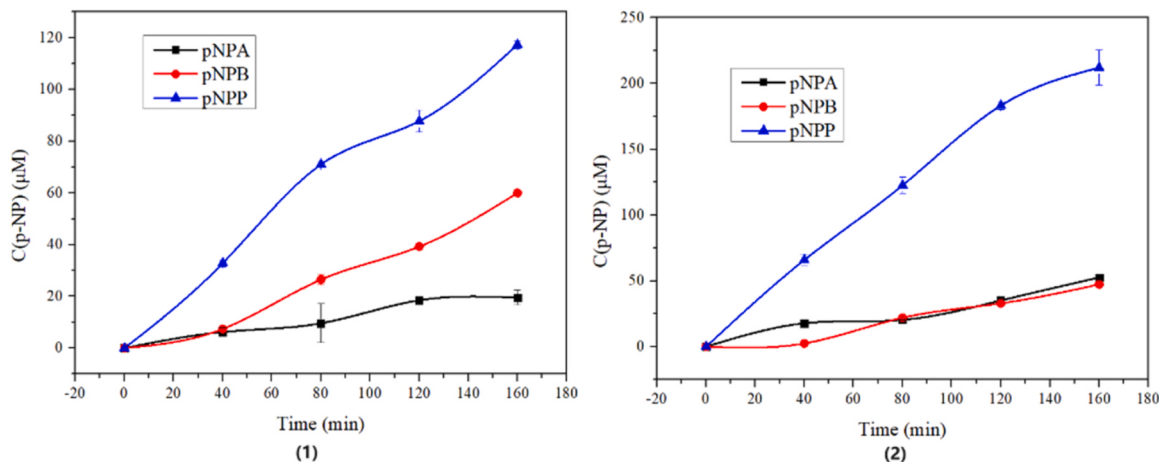


**Fig. 2.** Catalytic activities of HP in the hydrolysis of various substrates with different concentrations. (1: activities determined with 25 mM substrates; 2: activities determined with 50 mM substrates).

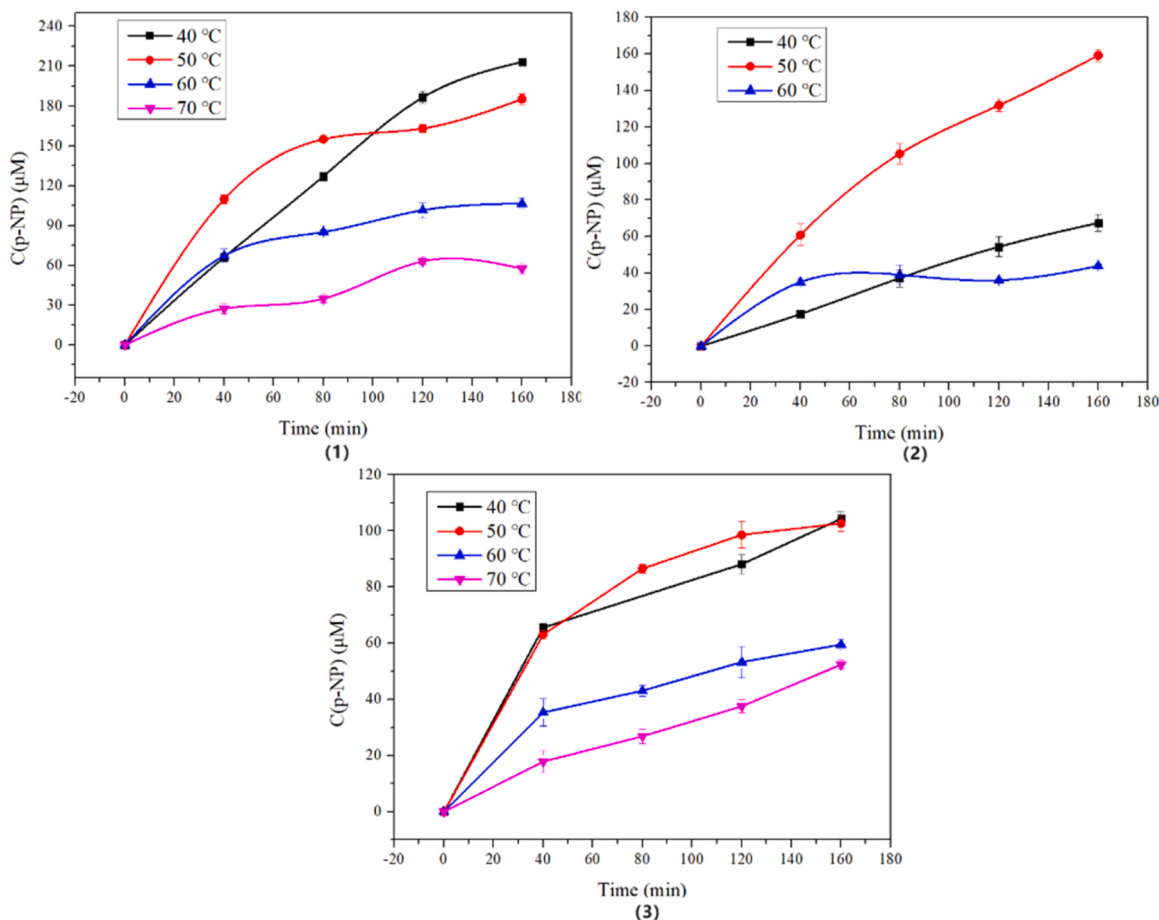


**Fig. 3.** Effect of different reaction temperatures on the catalytic performance of HP (1), HLCB (2) and D-HLCB (3) for the hydrolysis of p-NPP. (the HP and HLCB used in this study were crude enzymes; the final OD<sub>600</sub> of the D-HLCB cells used for enzymatic PET degradation was 0.49.).

different reaction temperatures (40, 50, and 60 °C) revealed that HP is a robust catalyst with increased longevity at 40 °C. Although an increased reaction temperature improves catalytic performance (Bell et al., 2022), it inevitably decreases enzyme stability, leading to decreased catalytic activity. Therefore, it is necessary to further improve the operational stability.

As shown in Fig. 3(2,3), the adsorption time courses of HLCB and D-HLCB were investigated at various temperatures. At 50 °C, the

maximum yield of the released products was achieved after ~160 min of incubation, with the highest conversion rate of 22.31 %. With increasing (or decreasing) incubation temperature to 60 °C, the maximum conversion rate decreased to 6.13 % after 2 h of incubation. Therefore, 50 °C is the optimal reaction temperature for HLCB-catalysed plastic degradation. The optimal temperatures for HLCB and D-HLCB were 10 °C greater than that for HP (40 °C). On the one hand, this could occur because HP is a relatively thermostable variant of IsPETase, which was

consistent with previous findings (Bell et al., 2022). This finding is similar to the improved optimal reaction temperature of fusion proteins ( $\text{LCC}^{\text{ICCG}}\text{-TrCBM}$  and  $\text{CfCBM-LCC}^{\text{ICCG}}$ ) (Chen et al., 2023). On the other hand, it was estimated that the direct interactions between the fused CBMs and PETase might contribute to the increased thermostability. The underlying mechanism is investigated in the following sections.

In addition, (Fig. 3(3)) temperature had different effects on the catalytic activity of D-HLCB and HLCB. No significant changes were observed at relatively high temperatures (40–50 °C), although increasing the temperature slightly improved the enzymatic activity. However, at higher reaction temperatures (60–70 °C), the degradation activity was significantly inhibited. This difference might result from the improved catalytic performance of the cell-surface displayed protein, and the cell surface might provide natural protection from higher ambient temperatures. On the other hand, enzymes immobilized on the cell surface might be structurally stable and resistant to the effects of extreme heat.

### 3.2.1. Thermostabilities of HP, HLCB, and D-HLCB

Thermostability plays a critical role in the catalytic performance of PETase, especially in industrial applications. As shown in Fig. 4, the stabilities of the PETase-associated enzymes decreased markedly at higher reaction temperatures, such as 60 °C or 70 °C. For example, at 70 °C after heat treatment for 2 h, only ~50.2%, 65.2%, and 7.65% of the initial activities of HP, HLCB and D-HLCB, respectively, were maintained. It was further confirmed that the BaCBM utilized probably increases the resistance of the fused protein to higher temperatures. The potential mechanisms underlying the increased thermostability of HLCB

were investigated in the following section.

Further investigations revealed that the whole-cell catalyst D-HLCB had the poorest stability. This is a strange phenomenon for an immobilized enzyme. The cell debris resulting from heat treatment might account for the decreased catalytic activity of D-HLCB rather than the disruption of PETase by heat treatment. The cell surface on which HLCB was displayed was disrupted by high-temperature processing. The released cell debris further covers a large proportion of the enzyme surface and may have a critical impact on the reduced catalytic performance. The PET-binding reaction catalysed by CBM and the PET-degradation catalysed by PETase occur on the enzyme surface. Therefore, the whole-cell catalyst with D-HLCB displayed on the cell surface was more likely to be inhibited by heat treatment.

### 3.2.2. Study on the effects of CBM on the thermostability of PETase

It was reported that spatial arrangement might play affect the catalytic performance of fusion catalysts, and the stimulatory effect disappears when the CBM domain is connected to the N-terminus of IsPETase<sup>EHA</sup> (Dai et al., 2021). Therefore, it is reasonable to speculate that the fused CBM directly contributes to the improved thermostability by increasing the interactions with the PETase.

To investigate this hypothesis, the structure of the fusion protein (HLCB) was constructed with MODELER. The interactions between the fused linker-CBM and PETase are simulated with flexible docking, and the best interaction modes are obtained based on the lowest docking energy with reasonable spatial configuration. The detailed interactions are highlighted in Fig. 5. The fused CBM is located on the surface of PETase and can directly interact with critical residues in the  $\alpha$ 7 helices

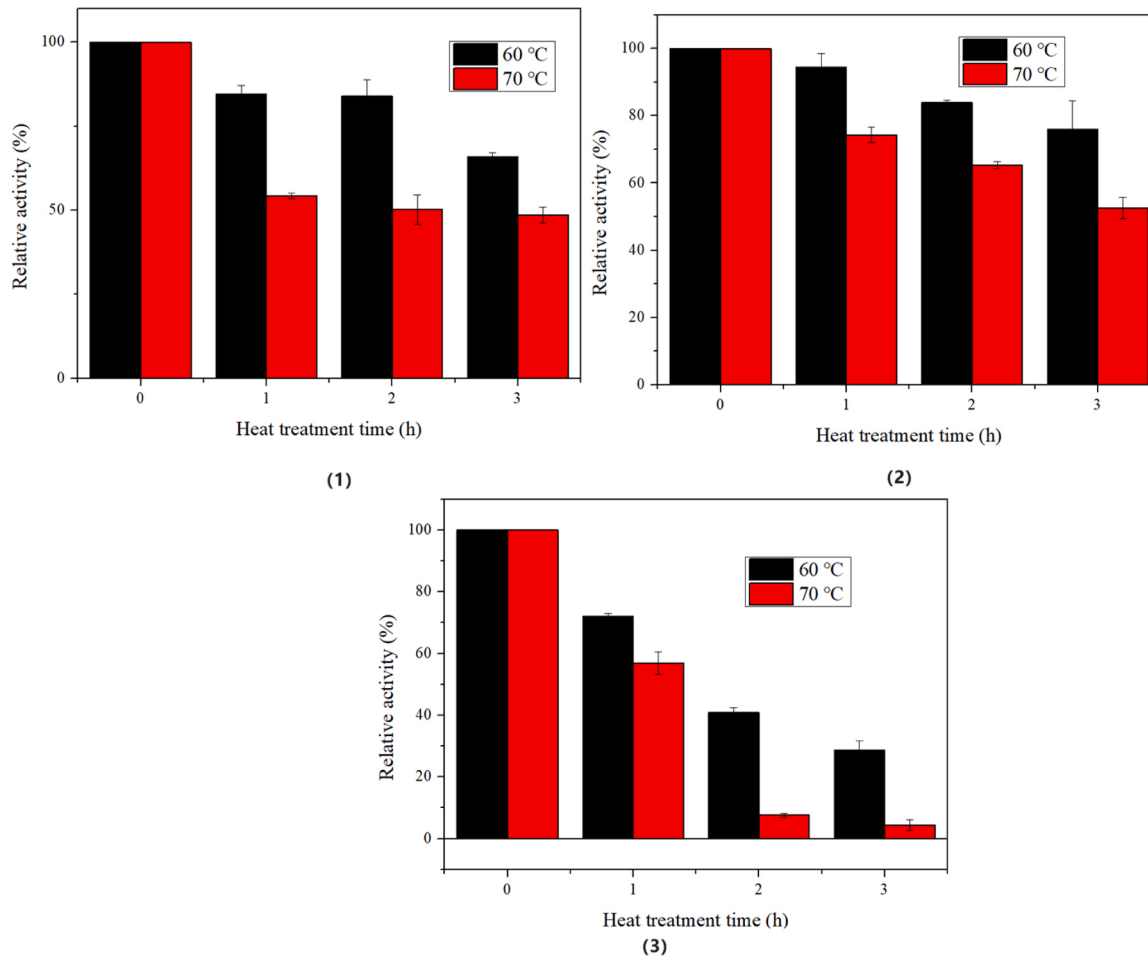


**Fig. 4.** Effects of heat treatment on the catalytic performance of HP (1), HLCB (2) and D-HLCB (3).

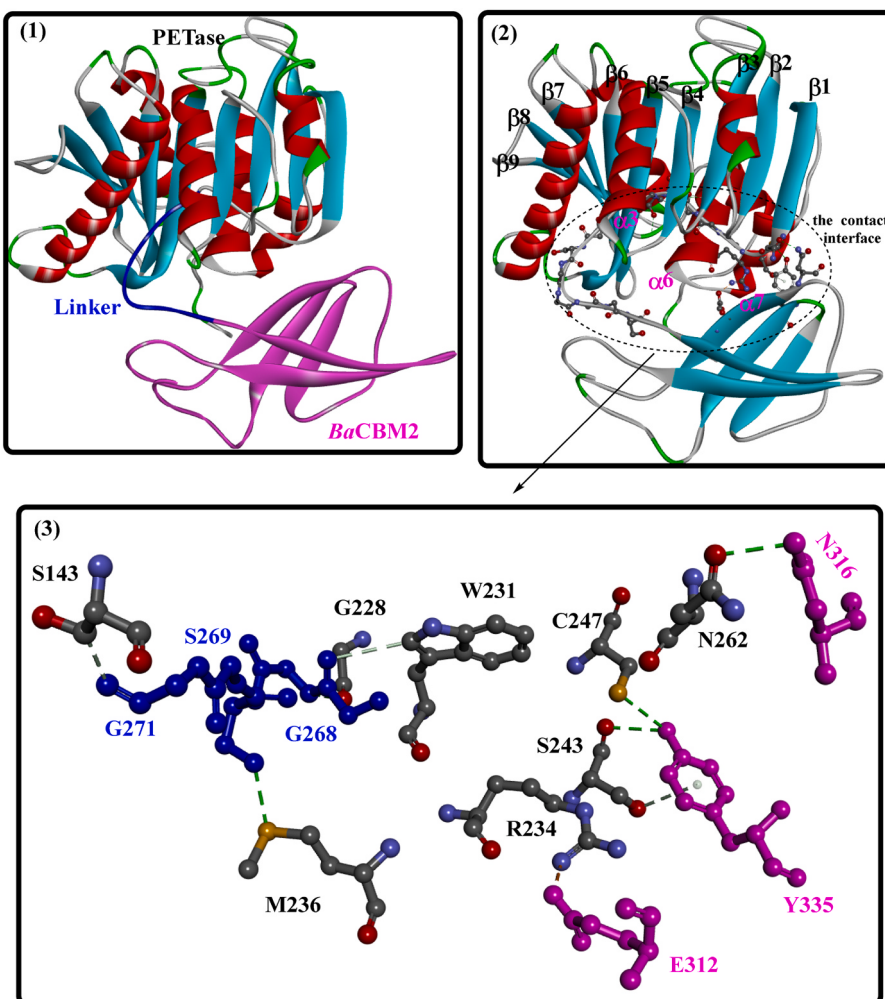


**Fig. 5.** Interactions between the HotPETase and the BaCBM2 simulated with DS. (1: the crystal structure of HLCB; 2: the contact interface between the HotPETase and the BaCBM2; 3: the detailed interactions between the HotPETase and the BaCBM2. The green dotted lines indicate the formed H-bonds; the purple dotted lines indicate the formed salt bridge; the gray dotted lines indicate the hydrophobic interactions).

(S243 and C247),  $\alpha$ 6 helices (R234) and  $\beta$ 1 helices (N262). Moreover, the linker sequence acts as a “zipper” located across  $\beta$ 4 and  $\beta$ 5, and it can interact with critical residues in the  $\alpha$ 3-helix (S143) and  $\alpha$ 6-helix (M236, W231, and G238). In particular, strong H-bonds could be formed between residues S269 and M236, G268 and G228, Y335 and C247, Y335 and S243, and N262 and N316. A salt bridge could also be formed between E312 and R234. These interactions not only provide physical protection but also further increase the structural rigidity of PETase, increasing its stability.

### 3.3. PET degradation catalysed by the constructed catalysts

#### 3.3.1. HLCB- and D-HLCB-mediated PET-mediated degradation

**3.3.1.1. HP.** Due to the special catalytic mechanism of HP, its potential applications could be extended to the biodegradation of PET waste, which can cause ubiquitous pollution. In this study, the use of PETase for the biodecomposition of widely used plastic bags (with low crystallinity) was investigated. As previously found (Bell et al., 2022; Wu, 2021), the reaction profile (Fig. 6(1), product accumulation over time) in this study was nonlinear, with a faster initial phase occurring after ~5 h and by a slower phase after 5–30 h.

The PET bags treated with HP (Fig. 6(1)) clearly degraded during the first 20 h, especially during the first 10 h, due to the increased catalytic stability of the HP. This finding corresponds with the biodegradation of

0.4 % cryPET substrate catalysed by HP (Bell et al., 2022). As revealed by the time course of reactions with HP, for reactions catalysed by HP, monomeric products can continue to accumulate for over 60 h. PET degradation probably ceased after ~70 h, maintaining an essentially constant yield of monomeric products (271.5  $\mu$ M after 71 h).

**3.3.1.2. HLCBs.** As shown in Fig. 6(2), the higher PET degradation rate was partly caused by the increased hydrophobic affinity towards PET; as the hydrophobic substrate binding surface was flatter than those of other PET-degrading enzymes (Joo et al., 2018). Therefore, the feasibility of using the carbohydrate-binding module to further improve PET degradation activity via the use of HP, which exhibits a higher affinity for PET substrates, was investigated.

Compared to the HP, HLCB exhibited relatively lower degradation activity in the first 20 h; however, the catalytic activity rapidly increased beginning at approximately 25 h. After 50 h, the yield of monomeric products (255.7  $\mu$ M) generated by HLCB was ~25.5 % greater than that obtained from HP-catalysed PET degradation (203.7  $\mu$ M). These findings are consistent with previous results showing that more time is needed for CBMs or hydrophobins to efficiently bind to the PET surface (Puspitasari et al., 2021a). If the assembly process is disrupted, the unwell-assembled CBMs will contribute little to the enhanced affinity of PETase for PET and stimulate the hydrolysis process. Therefore, it is reasonable that for the first ~20 h, HLCB displayed a relatively lower catalytic performance.

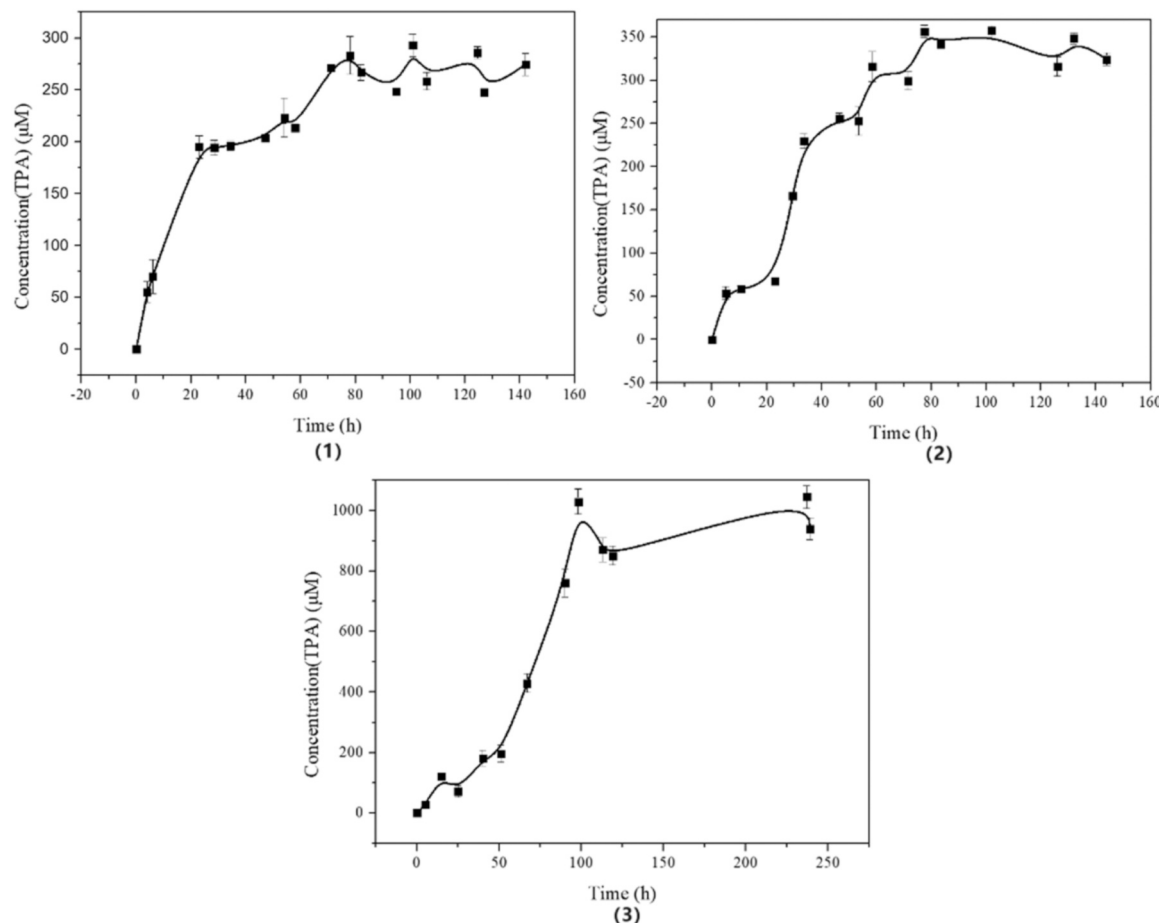


**Fig. 6.** PET degradation catalysed by HP, HLCB and D-HLCB. The concentrations of HP and HLCB were 230  $\mu\text{g}/\text{ml}$  and 25.9  $\mu\text{g}/\text{ml}$ , respectively; the final OD<sub>600</sub> of the D-HLCB cells used for enzymatic PET degradation was 7.93.

Interestingly, fusing CBMs onto the C-terminus of HP had a stimulatory effect on the enzymatic hydrolysis of PET. However, after  $\sim 60$  h, the PET depolymerization rate clearly decreased, which was attributed to the decreased operational stability. Although the accumulation of monomeric products might terminate after  $\sim 80$  h, the enzymatic PET degradation catalysed by HLCB was prolonged and increased by approximately 10 hours. The catalytic performance of HLCB increased by  $\sim 11.1$ -fold from 0.89  $\mu\text{M}$  (monomeric products)/protein ( $\mu\text{g}/\text{ml}$ ) to 9.87  $\mu\text{M}/\text{protein}$  ( $\mu\text{g}/\text{ml}$ ). This difference might be caused by the increased thermostability.

These findings suggest that fusing a polymer-binding module to PET-degrading catalysts is a promising strategy for stimulating the enzymatic hydrolysis of PET.

**3.3.1.3. D-HLCB.** *E. coli* cells that contained the HLCB expression system were coincubated with PET film from waste PET bags, and the results further highlighted the roles of fused CBMs in PET biodegradation. The fused CBMs could act on PET substrates, contributing to the efficient degradation of PETase; these effects might result from the colonized CBMs on the PET surface, which lead to higher concentrations of PETase and better contact on the PET film.

Similar to the reaction catalysed by HLCB, a longer time is needed for the CBMs to efficiently react with the PET surface, which leads to slower initial degradation ( $\sim 25$  h, Fig. 6(3)). Subsequently, PET depolymerization dramatically increased as the released products accumulated faster and increased in concentrations over time. The highest yield of monomeric products was up to 1.03 mM. Moreover, D-HLCB could maintain PET-degrading activity after  $\sim 100$  h, which was further increased by  $\sim 20$  hours compared with that of HLCB. This revealed that

the stability of the displayed PETase might also be improved.

### 3.3.2. Reusability of the whole-cell catalyst D-HLCB

The reusability of catalysts plays a critical role in reducing costs for industrial applications. In this study, the number of cycles in the D-HLCB system was investigated. The results (Fig. 7) showed that the displayed PET-degrading catalysts on the surface of *E. coli* cells could continuously maintain degradation activity. The residual activity of the D-HLCB system revealed a relatively low loss of PET-degrading activity during the

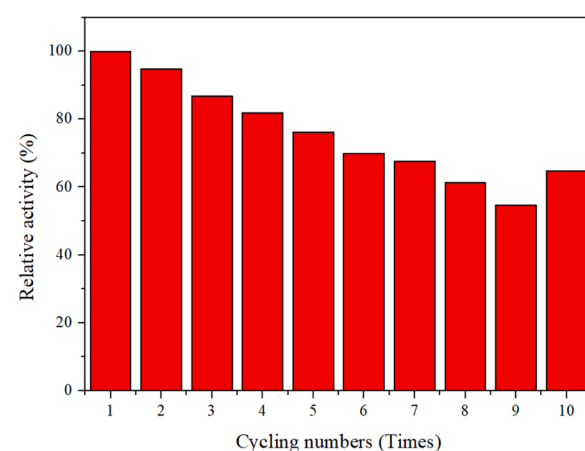


**Fig. 7.** Effect of recycling times on the catalytic performance of the whole-cell catalyst D-HLCB.

recycling process, and 54.6 % of its initial activity was maintained after nine cycles. In particular, recovery of D-HLCB could be achieved with an inexpensive strategy by centrifugation or filtration from the reaction system. These results indicate that the constructed D-HLCB system has enhanced reusability and sustainability and shows great potential for further PET degradation.

### 3.4. Molecular insights into the catalytic mechanisms of HCLB

### 3.4.1. Investigation of the PET-binding mechanisms of CBMs

The noncatalytic domains widely present in polysaccharide-degrading enzymes can facilitate substrate recognition and binding. Although CBM binding is promiscuous, it helps enrich the enzyme on the substrate surface. Among the different CBMs, type A CBMs (e.g., *BaCBM2*) are surface-binding proteins that include members of families 1, 2a, 3, 5, and 10. They are usually characterized by their high ability to bind insoluble, highly crystalline polysaccharides (e.g., cellulose and

chitin). This process is largely promoted by the special platform-like binding site lined by several surface-exposed aromatic amino acid residues, especially the aromatic triad that consists of W9-W44-W63 (for BaCBM2, Fig. 8(1)) (Zhang et al., 2013).

Docking studies showed that 2-HE(MHET)<sub>4</sub> could readily enter the binding site of *BaCBM*, and the surrounding polar amino acids could interact with the PET surface mainly through  $\pi$ -stacking interactions (shown as pink dotted lines) and H-bonds (shown as green lines) (Fig. 8 (2, 3, 4)). The roles of W288 and W323 in PET binding were confirmed in this study. Residues W288, V322, I327, K326, W309, I306, I298, K299, and L311 can form  $\pi$ -stacking interactions with PET; in addition, G291, Y292, Q321, S325, K326, K299 and I296 can form H-bonds with the PET surface. However, the initial binding of W342 to PET was not identified. This difference might occur because the initial binding of PET likely induces a structural rearrangement of *BaCBM*, resulting in simultaneous access of W342 and N343 to the PET surface (Weber et al., 2019; Rennison et al., 2023). Therefore, W342 might be a potential

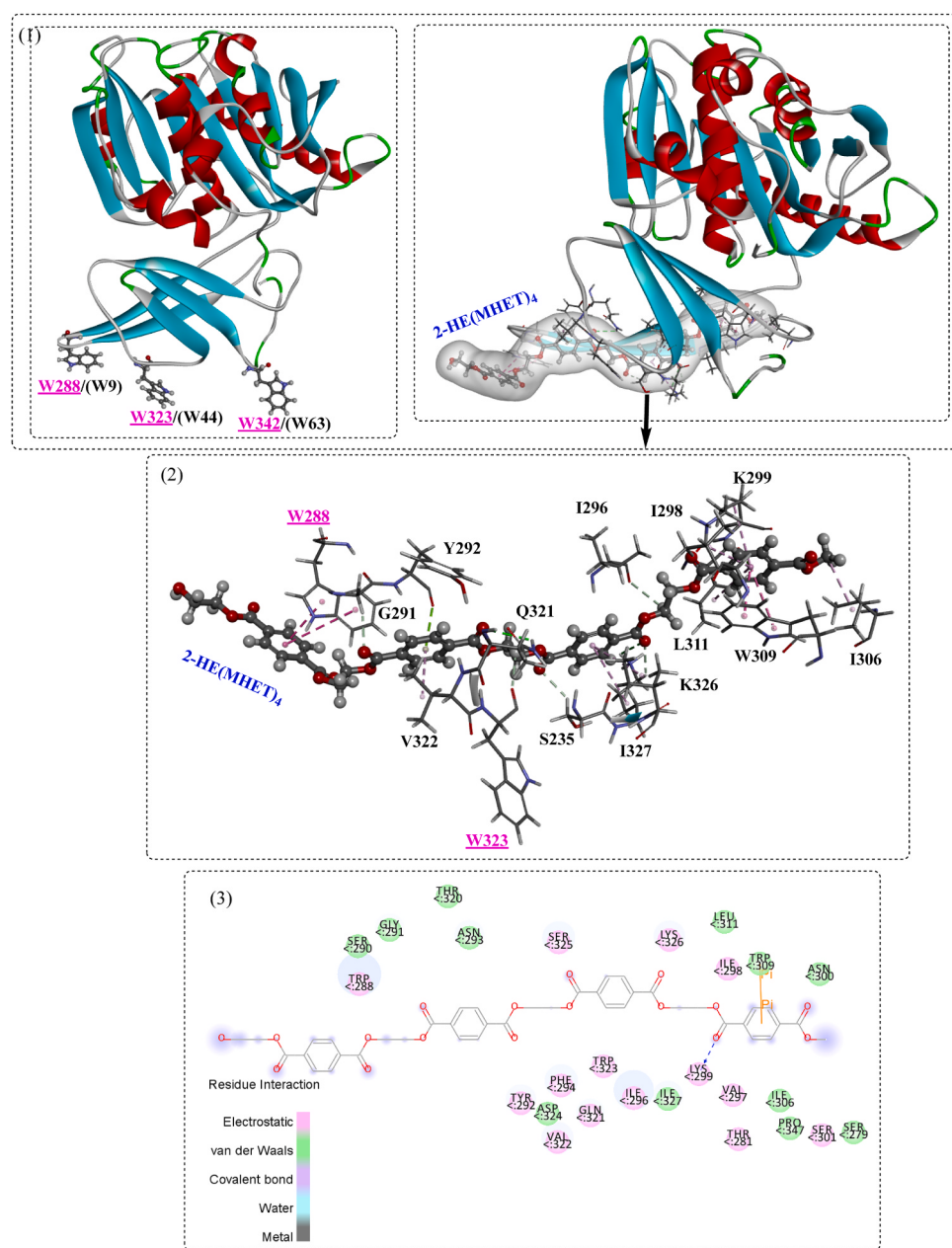


**Fig. 8.** The substrate binding mechanism of BaCBM was investigated by molecular docking.

target for performing site-directed mutagenesis to improve the affinity of BaCBM for the PET surface (Rennison et al., 2023).

### 3.4.2. Docking studies of the PET-degrading mechanisms of HP

*Is*PETases belong to the  $\alpha/\beta$  hydrolase superfamily, and the central twisted  $\beta$ -sheet is formed by 9 mixed  $\beta$ -strands and surrounded by 7  $\alpha$ -helices (Joo et al., 2018). As expected, *Is*PETase also contains the highly conserved serine hydrolase G-X1-S-X2-G motif (G158-W159-S160-M161-G162), which is located at the active site.

The catalytic activity and thermostability of PETase are closely linked to its structural effects, such as its conformation and different folded/native states. On the other hand, although crystal structures of different PETases or complex structures with monomeric products (e.g., HEMT [PDB ID: 5XH3]) have already been described, relatively few detailed structures that illustrate the degradation process of PET substrates are available. To gain further insight into the potential functionalities, especially the structural roles, of PETase and CBMs, molecular docking simulations were carried out with the 2-HE(MHET)<sub>4</sub> molecule as the ligand. The residues lining the binding cleft residues were set as flexible during the docking simulations.

As shown in Fig. 9(A), the polymer chain 2-HE(MHET)<sub>4</sub> of PET could suitably stretch to fill the substrate binding cleft (PETase) across the protein surface, and the TPA moiety could bind to the active site in a way

similar to the MHET complex structure of a cutinase from *Thermobifida fusca* (Yang et al., 2023b; Zeng et al., 2022). At the active site, the TPA moiety is located exactly immediately above the catalytic triad formed by S160, H237, and D206. In addition, the substrate in the long binding cleft could be further stabilized by different interactions. The TPA moiety is stabilized by hydrophobic interactions (formed with I208 and A89, shown as pink dotted lines in Fig. 9(B)) and weak H-bonding (formed with Y87, shown as a light green dotted line in Fig. 9(B)). The aliphatic part is mainly maintained by H-bond interactions formed with C233, G234, S245, S242, and G243, especially 2 strong H-bonds formed with S92 (Fig. 9(B)). Through these interactions, the whole polymer chain could be tightly bound to the active site.

As shown in Fig. 10(A), this binding cleft may accommodate as long as four monomers, 2-HE(MHET) (2-HE(MHET)<sub>4</sub>). Therefore, PET- might be biodegraded in an '*endo*' way catalysed by PETase, similar to the functions of TfCut, which first causes random cleavage of the side chains that enter the binding cleft. Once the smaller degrading intermediates (e.g., 2-HE(MHET)<sub>4</sub>, 2-HE(MHET)<sub>4</sub>, and MHET) are released, the "*exo*-reaction" could further catalyse the hydrolysis of the produced intermediates into various monomeric products, such as MHET, TPA, and EG.

To investigate the abovementioned mechanism of PETase degradation, MHET and 2-HE(MHET)<sub>2</sub> were chosen as substrate mimics for use

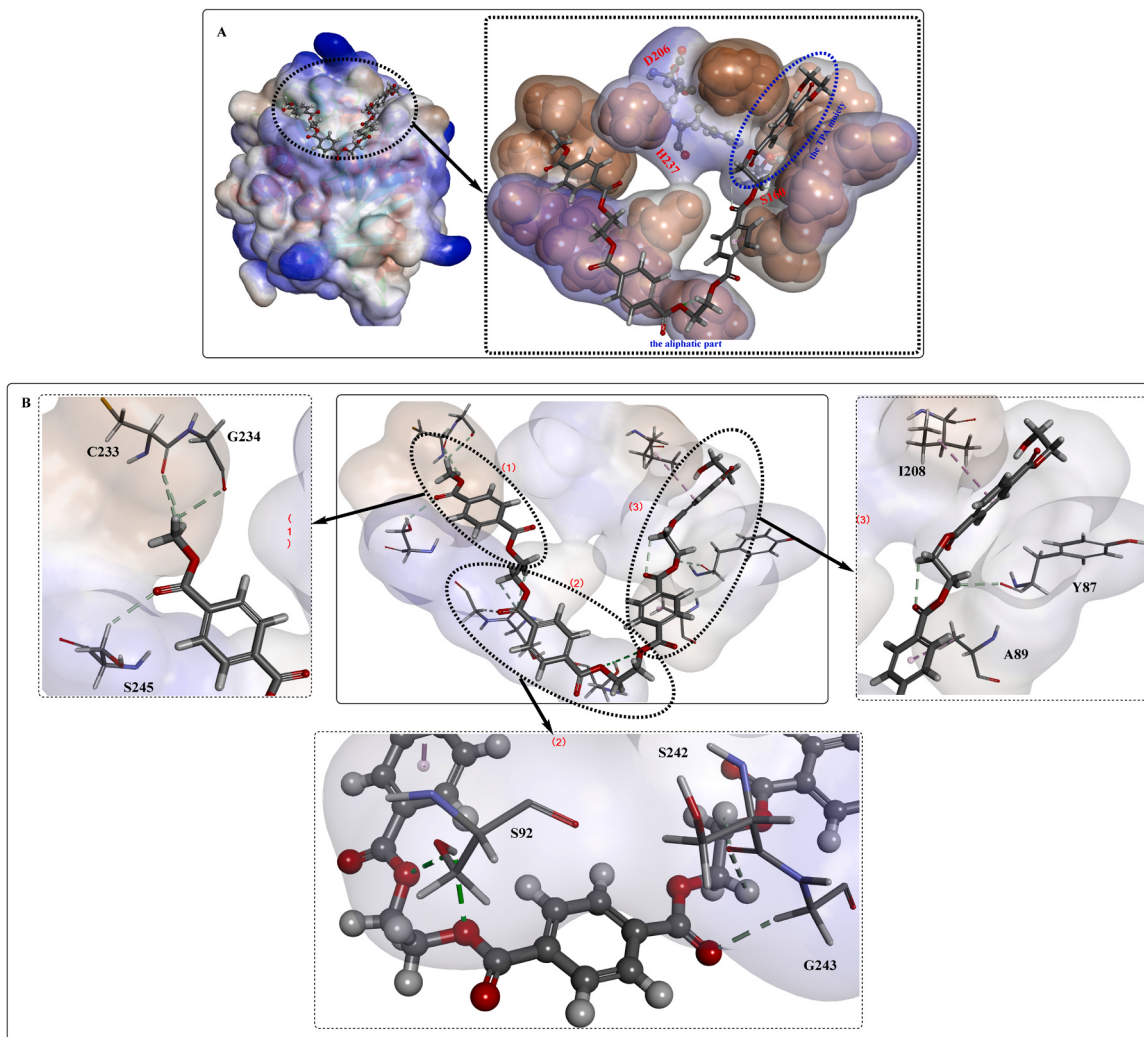


**Fig. 9.** The predicted binding mode of the polymer chain (2-HE(MHET)<sub>4</sub>) of PET in the active site tunnel of PETase, generated by flexible docking using Discovery Studio. ((A); B: Predicted interaction modes of 2-HE(MHET)<sub>4</sub>, generated and analysed using Discovery Studio (B): the detailed interactions of substrate in the different regions of the binding site).

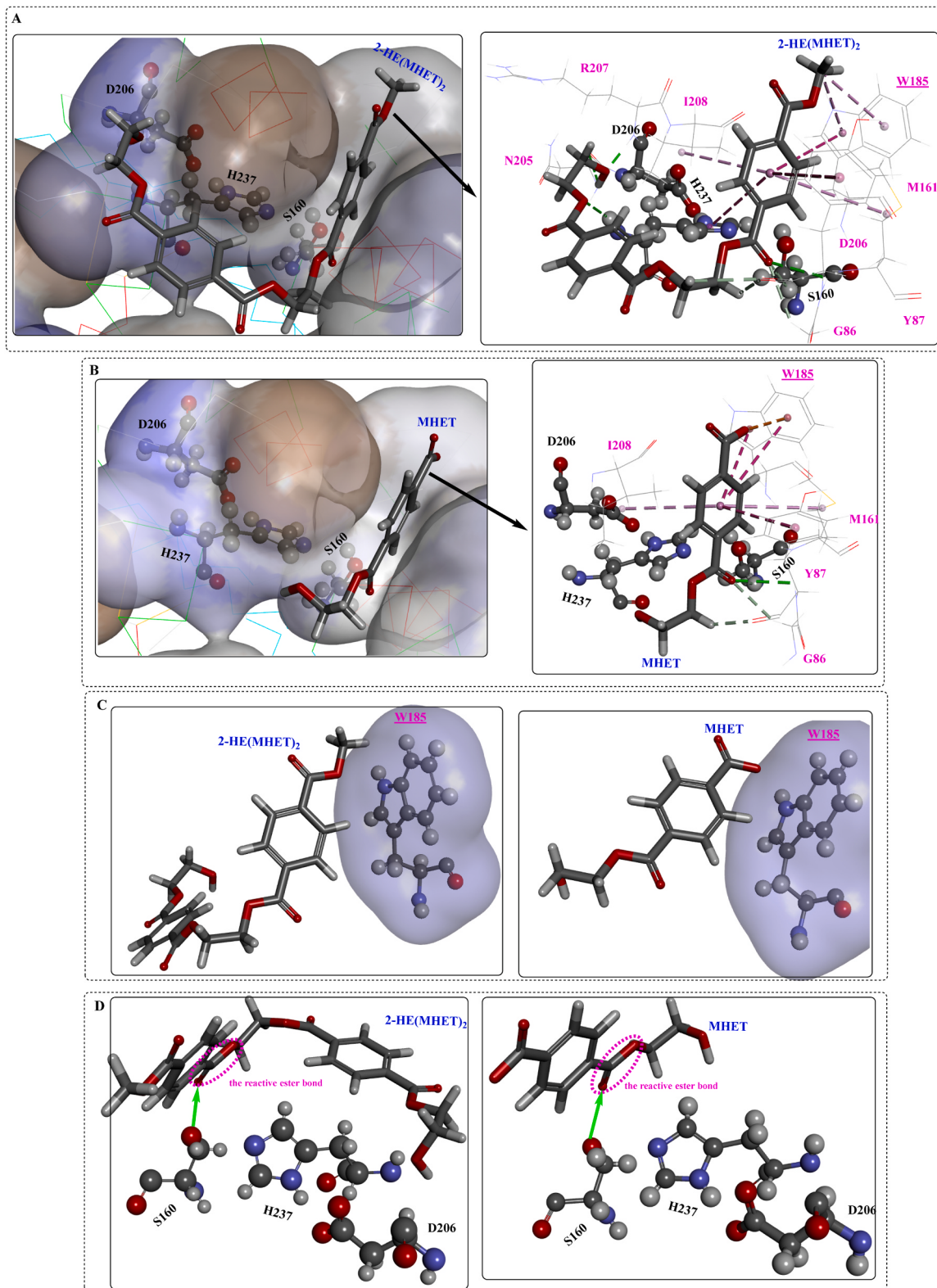


**Fig. 10.** The predicted binding mode and interactions of the polymer chain 2-HE(MHET)<sub>2</sub> of PET in the active site of PETase (A); B: Predicted interaction modes and interactions of MHET in the active site of PETase (B). All the results were generated and analysed using Discovery Studio.

in the following study. The docking results revealed that the binding modes of MHET (Fig. 10(B)) and 2-HE(MHET)<sub>2</sub>, which were bound to the binding cleft, (Fig. 10(A)) proximal to the catalytic S160 were similar to each other. The aromatic ring of the TPA moiety forms  $\pi$ -stacking interactions with W185, M161 and Y87 (shown as pink dotted lines);

moreover, the carbonyl group of the reactive ester bond can form H-bonds with Y87 and G86. In particular, site-directed mutagenesis further demonstrated that Y87 dramatically influences PET degradation (Han et al., 2017), which might be caused by a decreased substrate binding affinity, as mentioned above. Therefore, the results strongly suggested

that regulating hydrophobic amino acids (W185 and I208) to increase the openness of the PET-binding cleft and appropriate rotation of the side chain (especially the benzene ring) of Y87 would improve the catalytic activity, which might further improve the PET-degrading performance of PETase.

In addition, the interaction mode of 2-HE(MHET)<sub>2</sub> revealed that hydroxy and the second ester bond could also form H-bond interactions with R207 and N205 (Fig. 10(A)). W185 functions as a “gatekeeper”, and the orientation of its side chain plays a critical role in accommodating the longer chains of PET substrates (Fig. 10(C)). The results also revealed that regulating the flexibility of the W185 region (Liu et al., 2022) contributes to the catalytic performance of the DuraPETase<sup>N233C/S282C/H214S/S245R</sup> mutant. Furthermore, it was found that the segment around the active site (R171, N186, F218, S214, D186) plays critical roles in regulating the degradation activity and thermostability of PETase (Joho et al., 2023; Chen et al., 2021b), possibly through “W185 wobbling” and  $\beta$ 6- $\beta$ 7 loop flexibility.

Like that of carboxylesterases, protonated S160 of PETase should function as a covalent nucleophile for the carbonyl carbon atom in the scissile ester bond (Liu et al., 2023), and this initial acylation may be the rate-limiting step for the catalytic process of PETase (Boneta et al., 2021). In addition, a study indicated that the initial acylation and final deacylation steps (substrate release) might be the competing rate-limiting steps (Feng et al., 2021). As shown by the docking studies (Fig. 10(D)), MHET and 2-HE(MHET)<sub>2</sub> are very stable in the active site, and their reactive ester bonds are directly related to the catalytic S160. This binding pose facilitates an attack of the active ester bond by the catalytic residue S160.

Based on these findings, the PET-degrading activity of PETase could be improved by site-directed mutagenesis to rationally shorten the distance between the carbonyl carbon atom of the reactive ester bond and the hydroxy oxygen of the catalytic S160. However, this might result in unexpected consequences for the hydrophobic substrate-binding pocket.

#### 4. Conclusions

PET-plastics have been widely applied in daily life as storage materials and synthetic fabrics. However, resistance to chemical and biological degradation has led to the rapid accumulation of PET wastes in terrestrial and marine ecosystems at a terrifying rate. Recently, numerous efforts have been dedicated to alleviating this problem through the enzymatic hydrolysis of PETase-mediated PET degradation. In this study, a promising *IsPETase* mutant (HP) was applied for efficient PET biodegradation, which should be amenable to industrial application at mild temperature. The carbohydrate-binding module fused to PETase was further confirmed to improve the degradation of PET, including its catalytic activity and thermostability. However, the detailed mechanism responsible for the increased thermostability should be further investigated. Moreover, the whole-cell biocatalyst D-HLCB was shown to exhibit high thermal stability and high PET degradation activity. In particular, the HLCB displayed on the surface of *E. coli* could be used to efficiently degrade PET through enzymatic catalysis. Moreover, D-HLCB was shown to display good reusability and stability and could maintain more than 50 % of its initial activity for 9 cycles. This whole-cell catalyst shows great potential for providing an economical and efficient approach for the industrial biodegradation of PET waste.

Moreover, we elucidated the substrate-binding mechanisms and potential degradation mechanisms of PETase, and the critical residues associated with these biological processes were also identified. It is strongly believed that this structural information could be very effectively utilized in rational molecular engineering of PETase to further improve its thermal stability and PET degradation activity, which would provide opportunities for further industrial biodegradation of PET waste.

#### CRediT authorship contribution statement

**Tao Wang:** Writing – review & editing, Supervision, Project administration, Funding acquisition, Conceptualization. **You-shuang Zhu:** Supervision, Project administration, Investigation, Funding acquisition. **Xiao-huan Liu:** Writing – original draft, Project administration, Methodology, Investigation. **Fei Liu:** Writing – original draft, Project administration, Investigation, Funding acquisition. **Zhen-huan Lu:** Software, Resources, Methodology, Investigation. **Guo-cheng wang:** Methodology, Investigation, Formal analysis, Data curation. **Xin-xin Fan:** Methodology, Investigation, Formal analysis, Data curation. **Ying-kang Zhang:** Methodology, Investigation, Formal analysis, Data curation. **Yu-ming Gong:** Methodology, Investigation, Formal analysis, Data curation. **Wen-tao Yang:** Methodology, Investigation, Formal analysis, Data curation.

#### Declaration of Competing Interest

We wish to confirm that there are no known conflicts of interest associated with this publication and the financial support for this work have been given in the manuscript.

#### Data Availability

Data will be made available on request.

#### Acknowledgements

The authors express their gratitude to the Traditional Chinese Medicine Science and Technology Project of Shandong Province (M-2023080), the Shandong Provincial University Youth Innovation Team, China (No. 2022KJ102), the Research Fund for Academician Lin He New Medicine (JYHL2021MS23) and the National Natural Science Foundation of China (No. 32000194).

#### References

- Bell, E.L., Smithson, R., Kilbride, S., 2022. Directed evolution of an efficient and thermostable PET depolymerase. *Nat. Catal.* 5 (8).
- Boneta, S., Arafet, K., Moliner, V., 2021. QM/MM study of the enzymatic biodegradation mechanism of polyethylene terephthalate. *J. Chem. Inf. Model.* 61 (6), 3041–3051.
- Brandenberg, O.F., Schubert, O.T., Kruglyak, L., 2022. Towards synthetic PET trophy: engineering *pseudomonas putida* for concurrent polyethylene terephthalate (PET) monomer metabolism and PET hydrolase expression. *Microb. Cell Factor.* 21 (1), 119.
- Cao, F., Wang, L., Zheng, R., Guo, L., Chen, Y., Qian, X., 2022. Research and progress of chemical depolymerization of waste PET and high-value application of its depolymerization products. *RSC Adv.* 12 (49), 31564–31576.
- Carniel, A., Waldow, V.A., Castro, A.M., 2021. A comprehensive and critical review on key elements to implement enzymatic PET depolymerization for recycling purposes. *Biotechnol. Adv.* 52, 107811.
- Chen, C.C., Han, X., Li, X., Jiang, P., Guo, R.T., 2021b. General features to enhance enzymatic activity of poly(ethylene terephthalate) hydrolysis. *Nat. Catal.* 4 (5), 425–430.
- Chen, Y., Zhang, S., Zhai, Z., Zhang, S., Ma, J., Liang, X., Li, Q., 2023. Construction of fusion protein with carbohydrate-binding module and leaf-branch compost cutinase to enhance the degradation efficiency of polyethylene terephthalate. *Int. J. Mol. Sci.* 24 (3).
- Chen, Z., Xiao, Y., Weber, G., Wei, R., Wang, Z., 2021a. Yeast cell surface display of bacterial PET hydrolase as a sustainable biocatalyst for the degradation of polyethylene terephthalate. *Methods Enzymol.*
- Chen, Z., Duan, R., Xiao, Y., Wei, Y., Zhang, H., Sun, X., Wang, S., Cheng, Y., Wang, X., Tong, S., Yao, Y., Zhu, C., Yang, H., Wang, Y., Wang, Z., 2022. Biodegradation of highly crystallized poly(ethylene terephthalate) through cell surface codisplay of bacterial PETase and hydrophobin. *Nat. Commun.* 13 (1), 7138.
- Cui, L., Qiu, Y., Liang, Y., Du, C., Dong, W., Cheng, C., He, B., 2021b. Excretory expression of *IsPETase* in *E. coli* by an enhancer of signal peptides and enhanced PET hydrolysis. *Int. J. Biol. Macromol.* 188, 568–575.
- Cui, Y., Chen, Y., Liu, X., et al., 2021. Computational redesign of a PETase for plastic biodegradation under ambient condition by the GRAPE strategy[J]. *ACS Catalysis* 11 (3), 1340–1350.
- Dai, L., Qu, Y., Huang, J.W., Hu, Y., Hu, H., Li, S., Chen, C.C., Guo, R.T., 2021. Enhancing PET hydrolytic enzyme activity by fusion of the cellulose-binding domain of cellobiohydrolase I from *Trichoderma reesei*. *J. Biotechnol.* 334, 47–50.

- Deng, B., Yue, Y., Yang, J., Yang, M., Xing, Q., Peng, H., Wang, F., Li, M., Ma, L., Zhai, C., 2023. Improving the activity and thermostability of PETase from *Ideonella sakaiensis* through modulating its post-translational glycan modification. *Commun. Biol.* 6 (1), 39.
- Ellis, L.D., Rorrer, N.A., Sullivan, K.P., Otto, M., Mcgeehan, J.E., Roman-Leshkov, Y., Wierckx, N., Beckham, G.T., 2021. Chemical and biological catalysis for plastics recycling and upcycling. *Nat. Catal.* 4 (7).
- Feng, S., Yue, Y., Zheng, M., Li, Y., Wang, W., 2021. Is PETase- and Is MHETase-catalyzed cascade degradation mechanism toward polyethylene terephthalate. *ACS Sustain. Chem. Eng.*
- Gao, R., Pan, H., Kai, L., Han, K., Lian, J., 2022. Microbial degradation and valorization of poly(ethylene terephthalate) (PET) monomers. *World J. Microbiol. Biotechnol.* 38 (5), 89.
- Gercke, D., Furtmann, C., Tozakidis, I.E.P., Jose, J., 2021. Highly crystalline post consumer PET waste hydrolysis by surface displayed PETase using a bacterial whole cell biocatalyst. *ChemCatChem.*
- Guo, F., Liu, M., Liu, H., Li, C., Feng, X., 2023. Direct yeast surface codisplay of sequential enzymes with complementary anchor motifs: enabling enhanced glycosylation of natural products. *ACS Synth. Biol.* 12 (2), 460–470.
- Han, X., Liu, W., Huang, J.W., Ma, J., Zheng, Y., Ko, T.P., Xu, L., Cheng, Y.S., Chen, C.C., Guo, R.T., 2017. Structural insight into catalytic mechanism of PET hydrolase. *Nat. Commun.* 8 (1), 2106.
- He, Z., Yang, X., Tian, X., Li, L., Liu, M., 2022. Yeast cell surface engineering of a nicotinamide riboside kinase for the production of β-nicotinamide mononucleotide via whole-cell catalysis. *ACS Synth. Biol.* 11 (10), 3451–3459.
- Joho, Y., Vongsouthi, V., Spence, M.A., Ton, J., Gomez, C., Tan, L.L., Kaczmarski, J.A., Caputo, A.T., Royan, S., Jackson, C.J., Ardevol, A., 2023. Ancestral sequence reconstruction identifies structural changes underlying the evolution of *Ideonella sakaiensis* PETase and variants with improved stability and activity. *Biochemistry* 62 (2), 437–450.
- Joo, S., Cho, I.J., Seo, H., Son, H.F., Sagong, H.Y., Shin, T.J., Choi, S.Y., Lee, S.Y., Kim, K., J., 2018. Structural insight into molecular mechanism of poly(ethylene terephthalate) degradation. *Nat. Commun.* 9 (1), 382.
- Kumar, V., Sharma, N., Duhan, L., Pasrija, R., Thomas, J., Umesh, M., Lakkaboyana, S.K., Andler, R., Vangnai, A.S., Vithanage, M., Awasthi, M.K., Chia, W.Y., LokeShow, P., Barceló, D., 2022. Microbial engineering strategies for synthetic microplastics clean up: a review on recent approaches. *Environ. Toxicol. Pharmacol.* 98, 104045.
- Liu, F., Wang, T., Yang, W., Zhang, Y., Fan, X., Wang, G., Lu, Z., Wang, J., 2023. Current advances in the structural biology and molecular engineering of PETase. *Front. Bioeng. Biotechnol.* 11, 1263996.
- Liu, Y., Liu, Z., Guo, Z., Yan, T., Jin, C., Wu, J., 2022. Enhancement of the degradation capacity of IsPETase for PET plastic degradation by protein engineering. *Sci. Total Environ.* 834, 154947.
- Lu, H., Diaz, D.J., Czarnecki, N.J., Zhu, C., Kim, W., Shroff, R., Acosta, D.J., Alexander, B. R., Cole, H.O., Zhang, Y., Lynd, N.A., Ellington, A.D., Alper, H.S., 2022. Machine learning-aided engineering of hydrolases for PET depolymerization. *Nature* 604 (7907), 662–667.
- Ma, Y., Yao, M., Li, B., Ding, M., Yuan, Y., 2018. Enhanced poly(ethylene terephthalate) hydrolase activity by protein engineering. *Engineering* 4 (6).
- Meng, X., Yang, L., Liu, H., Li, Q., Xu, G., Zhang, Y., Guan, F., Zhang, Y., Zhang, W., Wu, N., Tian, J., 2021. Protein engineering of stable IsPETase for PET plastic degradation by Premuse. *Int. J. Biol. Macromol.* 180, 667–676.
- Miri, S., Saini, R., Davoodi, S.M., Pulicharla, R., Brar, S.K., Magdouli, S., 2022. Biodegradation of microplastics: Better late than never. *Chemosphere* 286 (Pt 1) 0, 131670.
- Moyses, D.N., Teixeira, D.A., Waldow, V.A., Freire, D.M.G., Castro, A.M., 2021. Fungal and enzymatic bio-depolymerization of waste post-consumer poly(ethylene terephthalate) (PET) bottles using *Penicillium* species. *3 Biotech* 11 (10), 435.
- Pham, M.L., Polaković, M., 2020. Microbial cell surface display of oxidoreductases: concepts and applications. *Int. J. Biol. Macromol.* 165 (Pt A), 835–841.
- Pirillo, V., Orlando, M., Battaglia, C., Pollegioni, L., Molla, G., 2023. Efficient polyethylene terephthalate degradation at moderate temperature: a protein engineering study of LC-cutinase highlights the key role of residue 243. *FEBS J.* 290 (12), 3185–3202.
- Puspitasari, N., Tsai, S.L., Lee, C.K., 2021b. Fungal hydrophobin rola enhanced petase hydrolysis of polyethylene terephthalate. *Appl. Biochem. Biotechnol.* 193 (5), 1284–1295.
- Puspitasari, N., Tsai, S.L., Lee, C.K., 2021a. Class I hydrophobins pretreatment stimulates PETase for monomers recycling of waste PETs. *Int. J. Biol. Macromol.* 176, 157–164.
- Rennison, A.P., Westh, P., Moller, M.S., 2023. Protein-plastic interactions: the driving forces behind the high affinity of a carbohydrate-binding module for polyethylene terephthalate. *Sci. Total Environ.* 870, 161948.
- Ribitsch, D., Yebra, A.O., Zitzenbacher, S., Wu, J., Nowitsch, S., Steinkellner, G., Greimel, K., Doliska, A., Oberdorfer, G., Gruber, C.C., Gruber, K., Schwab, H., Stanak-Kleinschek, K., Aceri, E.H., Guebitz, G.M., 2013. Fusion of binding domains to *Thermobifida cellulosa* cutinase to tune sorption characteristics and enhancing PET hydrolysis. *Biomacromolecules* 14 (6), 1769–1776.
- Ribitsch, D., Herrero Acero, E., Przylucka, A., Zitzenbacher, S., Marold, A., Gamerith, C., Tscheließnig, R., Jungbauer, A., Rennhofer, H., Lichtenegger, H., Amenitsch, H., Bonazza, K., Kubicek, C.P., Druzhinina, I.S., Guebitz, G.M., 2015. Enhanced cutinase-catalyzed hydrolysis of polyethylene terephthalate by covalent fusion to hydrophobins. *Appl. Environ. Microbiol.* 81 (11), 3586–3592.
- Seo, H., Kim, S., Son, H.F., Sagong, H.Y., Joo, S., Kim, K.J., 2019. Production of extracellular PETase from *Ideonella sakaiensis* using sec-dependent signal peptides in *E. coli*. *Biochem. Biophys. Res. Commun.* 508 (1), 250–255.
- Shi, L., Liu, H., Gao, S., Weng, Y., Zhu, L., 2021. Enhanced extracellular production of IsPETase in *Escherichia coli* via engineering of the pelB signal peptide. *J. Agric. Food Chem.* 69 (7), 2245–2252.
- Shi, L., Liu, P., Tan, Z., Zhao, W., Gao, J., Gu, Q., Ma, H., Liu, H., Zhu, L., 2023. Complete depolymerization of PET wastes by an evolved PET hydrolase from directed evolution. *Angew. Chem. (Int. Ed. Engl.)* 62 (14), e202218390.
- Singh Jadua, J., Bansal, S., Sonthalia, A., Rai, A.K., Singh, S.P., 2022. Biodegradation of plastics for sustainable environment. *Bioresour. Technol.* 347, 126697.
- Son, H.F., Cho, I.J., Joo, S., Seo, H., Kim, K.J., 2019. Rational protein engineering of thermo-stable PETase from *Ideonella sakaiensis* for highly efficient PET degradation. *ACS Catal.* 9 (4).
- Son, H.F., Joo, S., Seo, H., Sagong, H.Y., Lee, S.H., Hong, H., Kim, K.J., 2020. Structural bioinformatics-based protein engineering of thermo-stable PETase from *Ideonella sakaiensis*. *Enzym. Microb. Technol.* 141, 109656.
- Tamargo, A., Molinero, N., Reinosa, J.J., Alcolea-Rodriguez, V., Portela, R., Bañares, M. A., Fernández, J.F., Moreno-Arribas, M.V., 2022. PET microplastics affect human gut microbiota communities during simulated gastrointestinal digestion, first evidence of plausible polymer biodegradation during human digestion. *Sci. Rep.* 12 (1), 528.
- Tamoor, M., Samak, N.A., Jia, Y., Mushtaq, M.U., Sher, H., Bibi, M., Xing, J., 2021. Potential use of microbial enzymes for the conversion of plastic waste into value-added products: a viable solution. *Front. Microbiol.* 12, 777727.
- Taniguchi, I., Yoshida, S., Hiraga, K., Miyamoto, K., Kimura, Y., Oda, K., 2019. Biodegradation of PET: current status and application aspects. *ACS Catal.* 9 (5), 4089–4105.
- Tissoppi, T., Kumar, S., Sadhu, A., 2022. Surface display of novel transglycosylating α-glucosidase from *Aspergillus neoniger* on *Pichia pastoris* for synthesis of isomaltoligosaccharides. *Biochem. Eng. J.*
- Tournier, V., Topham, C.M., Gilles, A., David, B., Folgoas, C., Moya-Leclair, E., Kamionka, E., Desrousseaux, M.L., Texier, H., Gavalda, S., Cot, M., Guérard, E., Dalibey, M., Nomme, J., Cioci, G., Barbe, S., Chateau, M., André, I., Duquesne, S., Marty, A., 2020. An engineered PET depolymerase to break down and recycle plastic bottles. *Nature* 580 (7802), 216–219.
- Urbanek, A.K., Kosirowska, K.E., Mironczuk, A.M., 2021. Current knowledge on polyethylene terephthalate degradation by genetically modified microorganisms. *Front. Bioeng. Biotechnol.* 9, 771133.
- von Haugwitz, G., Han, X., Pfaff, L., Li, Q., Wei, H., Gao, J., Methling, K., Ao, Y., Brack, Y., Mican, J., Feiler, C.G., Weiss, M.S., Bednar, D., Palm, G.J., Lalk, M., Lammers, M., Damborsky, J., Weber, G., Liu, W., Bornscheuer, U.T., Wei, R., 2022. Structural insights into (Tere)phthalate-ester hydrolysis by a carboxylesterase and its role in promoting PET depolymerization. *ACS Catal.* 12 (24), 15259–15270.
- Weber, J., Petrović, D., Strodel, B., Smits, S.H.J., Kolkenbroek, S., Leggewie, C., Jaeger, K.E., 2019. Interaction of carbohydrate-binding modules with poly(ethylene terephthalate). *Appl. Microbiol. Biotechnol.* 103 (12), 4801–4812.
- Wei, R., Zimmermann, W., 2017. Biocatalysis as a green route for recycling the recalcitrant plastic polyethylene terephthalate. *Microb. Biotechnol.* 10 (6), 1302–1307.
- Wu, Y.C.C. De.T.Q.M.H.L.H.L.C.W.W.D.T.X.L.N.H., 2021. Computational Redesign of a PETase for plastic biodegradation under ambient condition by the GRAPE strategy. *ACS Catal.* 11 (3).
- Yang, Y., Min, J., Xue, T., Jiang, P., Liu, X., Peng, R., Huang, J.W., Qu, Y., Li, X., Ma, N., 2023b. Complete bio-degradation of poly(butylene adipate-co-terephthalate) via engineered cutinases. *Nat. Commun.* 14.
- Yang, Y., Min, J., Xue, T., Jiang, P., Liu, X., Peng, R., Huang, J.W., Qu, Y., Li, X., Ma, N., Tsai, F.C., Dai, L., Zhang, Q., Liu, Y., Chen, C.C., Guo, R.T., 2023a. Complete bio-degradation of poly(butylene adipate-co-terephthalate) via engineered cutinases. *Nat. Commun.* 14 (1), 1645.
- Yin, Q., You, S., Zhang, J., Qi, W., Su, R., 2022. Enhancement of the polyethylene terephthalate and mono-(2-hydroxyethyl) terephthalate degradation activity of *Ideonella sakaiensis* PETase by an electrostatic interaction-based strategy. *Bioresour. Technol.* 364, 128026.
- Yoshida, S., Hiraga, K., Takehana, T., Taniguchi, I., Yamaji, H., Maeda, Y., Toyohara, K., Miyamoto, K., Kimura, Y., Oda, K., 2016. A bacterium that degrades and assimilates poly(ethylene terephthalate). *Science* 351 (6278), 1196–1199.
- Zeng, W., Li, X., Yang, Y., et al., 2022. Substrate-Binding Mode of a Thermophilic PET Hydrolase and Engineering the Enzyme to Enhance the Hydrolytic Efficacy[J]. *ACS catal* 12 (5).
- Zhang, Y., Wang, L., Chen, J., Wu, J., 2013. Enhanced activity toward PET by site-directed mutagenesis of *Thermobifida fusca* cutinase-CBM fusion protein. *Carbohydr. Polym.* 97 (1), 124–129.
- Zumstein, M.T., Rechsteiner, D., Roduner, N., Perz, V., Ribitsch, D., Guebitz, G.M., Kohler, H.E., McNeill, K., Sander, M., 2017. Enzymatic hydrolysis of polyester thin films at the nanoscale: effects of polyester structure and enzyme active-site accessibility. *Environ. Sci. Technol.* 51 (13), 7476–7485.
- Zurier, H.S., Goddard, J.M., 2023. A high-throughput expression and screening platform for applications-driven PETase engineering. *Biotechnol. Bioeng.* 120 (4), 1000–1014.